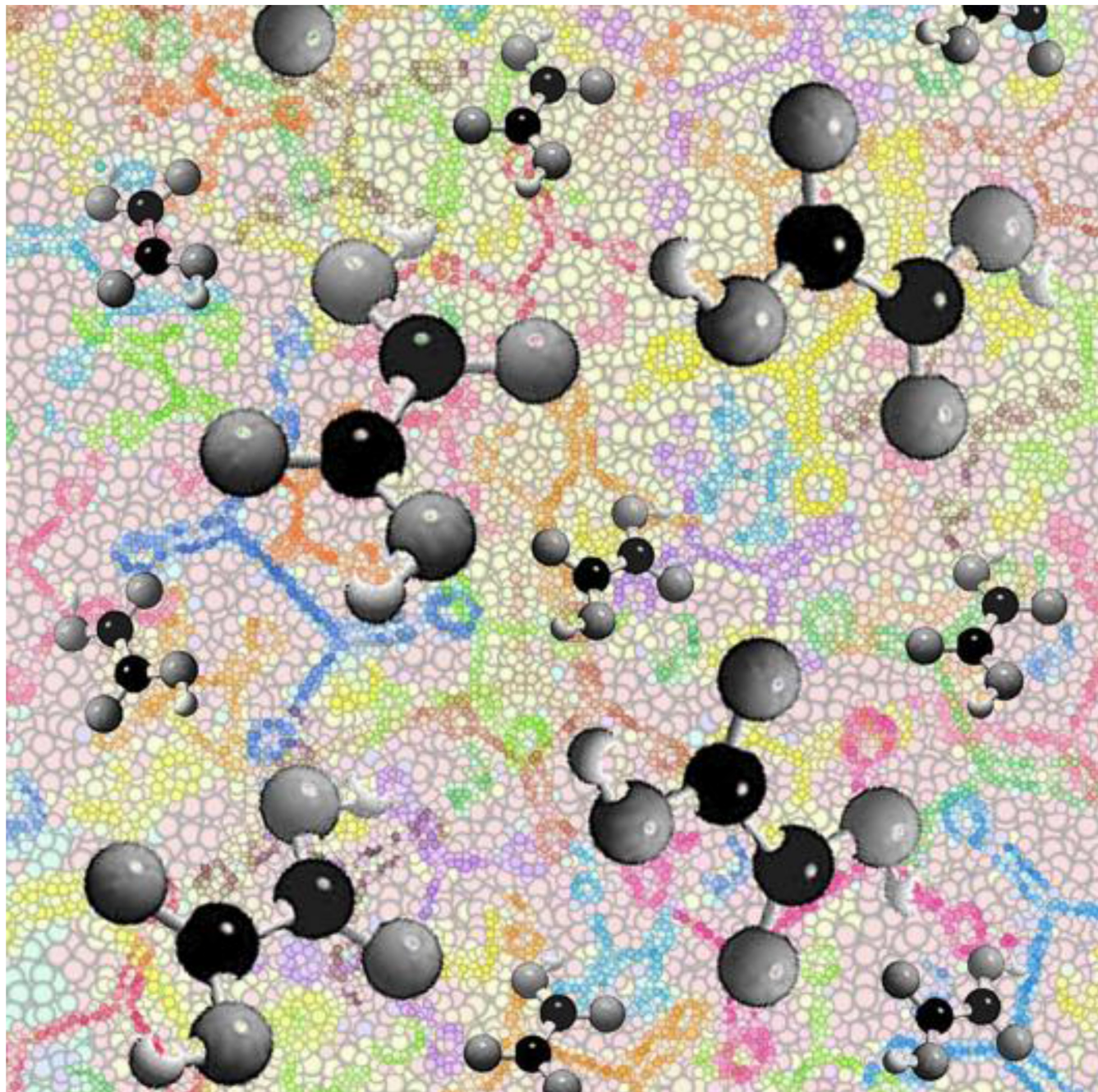


# The Multiple Facets of Oxalate Dianion in Photochemistry

Camilla Russo<sup>+, [a]</sup>, Carmine Volpe<sup>+, [a]</sup> and Mariateresa Giustiniano<sup>\*, [a]</sup>



Oxalate salts are cheap and available reagents used in organic photochemistry as C1-synthons, single-electron transfer (SET) reductants, and *hole* scavengers. Relying on these multiple

roles, a critical comparison of recent applications provides a roadmap to the diverse reductive functionalizations, highlighting the unmet challenges and the future developments.

## 1. Introduction

Oxalic acid (C<sub>2</sub>H<sub>2</sub>O<sub>4</sub>), known since the second half of the 18<sup>th</sup> century, is the simplest dicarboxylic acid, a relatively strong “weak” acid (pK<sub>a1</sub> = 1.25; pK<sub>a2</sub> = 3.81), whose name relates to *Oxalis* (wood-sorrels) plants.<sup>[1–4]</sup> Naturally occurring in fruits and vegetables, it is largely used in many industrial processes,<sup>[5]</sup> as a bidentate ligand in coordination chemistry (i.e., as a chelating and a precipitating agent), with one of the most representative applications being the anticancer drug oxaliplatin. Oxalic acid is also the most abundant dicarboxylic acid in the atmosphere and can influence clouds’ formation.<sup>[6]</sup> Recently, it has been suggested as a chemical intermediate for carbon capture and utilization.<sup>[7]</sup> In synthetic organic chemistry it has been shown that the oxidative fragmentation of oxalic acid dianion (C<sub>2</sub>O<sub>4</sub>)<sup>2-</sup> under visible light photo(redox) catalytic conditions affords carbon dioxide (CO<sub>2</sub>) and carbon dioxide radical anion (CO<sub>2</sub><sup>•-</sup>).<sup>[8]</sup> The latter is a strong single-electron transfer (SET) reductant (E<sub>1/2</sub> = -2.2 V vs SCE), whereas both CO<sub>2</sub> and CO<sub>2</sub><sup>•-</sup> can act as a C1-source.<sup>[9,10]</sup> It is worth noting that, given its redox potential, the direct SET reduction of CO<sub>2</sub> to CO<sub>2</sub><sup>•-</sup> is challenging, thus indicating oxalic acid dianion (E<sub>1/2</sub> = +0.06 V vs SCE) as the most convenient source of CO<sub>2</sub><sup>•-</sup>.<sup>[11]</sup> Alternatively, the latter can be formed upon hydrogen atom abstraction by means of a hydrogen atom transfer (HAT) agent from formate salts.<sup>[9,12]</sup> Oxalic acid is also a H-donor and a *hole* scavenger (in heterogeneous photocatalysis). The aim of the current article is to foreground oxalate salts as cheap and available reagents in synthetic organic photochemistry. Representative applications from recent literature are organized in different sections focused on: oxalate salts as CO<sub>2</sub><sup>•-</sup> precursors; oxalate salts in the formation of electron donor-acceptor (EDA) complexes; and oxalate salts as *hole* scavengers. A final section spotlights the UV photolysis of transition metal oxalate complexes. A comparative analysis of the mechanistic pathways draws the rationale to switch among different chemo-selective reactivity patterns.

## 2. Oxalate Salts as CO<sub>2</sub><sup>•-</sup> Precursors via Photoredox Catalysis

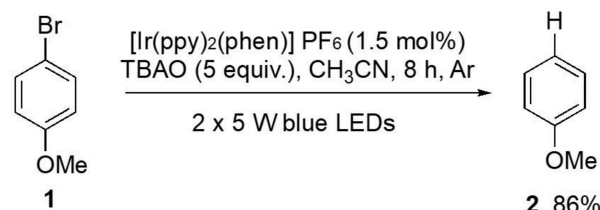
Pioneering studies reporting the formation of CO<sub>2</sub><sup>•-</sup> via oxidative decomposition of oxalate salts date back to the 80s of the last Century.<sup>[13]</sup> More recently, in 2018 and 2020, the groups of A. J. Bard and D. W. Bahnemann reported the generation of CO<sub>2</sub><sup>•-</sup> via either electro-oxidation or photo-oxidation of C<sub>2</sub>O<sub>4</sub><sup>2-</sup>, respectively. Early applications in organic synthesis rely, among others, on its use as a sacrificial electron donor to reduce methyl viologen.<sup>[11,14–17]</sup> In 2016, Y. You et al. harnessed [Ir-(dFppy)<sub>2</sub>(bpy)]PF<sub>6</sub> as a photoredox catalyst to generate CO<sub>2</sub><sup>•-</sup>, the latter acting as a co-reactant in the SET reduction of CF<sub>3</sub>I (E<sub>red</sub> = -0.91 V vs SCE) to generate, upon mesolytic fragmentation, the trifluoromethyl radical CF<sub>3</sub><sup>•</sup>.<sup>[18]</sup> Later on, in 2023, T. U. Connell et al. showed that the photoredox catalytic oxidative degradation of C<sub>2</sub>O<sub>4</sub><sup>2-</sup> enabled to exploit the highly reductive redox potential of CO<sub>2</sub><sup>•-</sup> in the reduction of aryl halides, including challenging substrates such as 4-bromoanisole (E<sub>p</sub> = -2.72 V vs SCE).<sup>[19]</sup> According to Scheme 1, anisole **2** was obtained in 68% yield with [Ir(ppy)<sub>2</sub>(phen)]PF<sub>6</sub> (1.5 mol%) as the photoredox catalyst and tetra-*n*-butylammonium oxalate (TBAO) as an organic soluble salt (5 equiv.).

The aryl halide reductions (9 examples, 86–99% yield) were run in acetonitrile as the solvent (0.05 M) and required irradiation with two 5 W blue LEDs (λ = 457 nm) for up to 8 h. It is worth noting that replacing the oxalate electron donor with triethylamine (TEA) led to 0% yield, probably due to the inability of TEA α-amino alkyl radical (E<sup>0</sup> ≈ -1.6 V vs SCE) to engage such challenging substrates.<sup>[20]</sup> Later on, J. Wu and Y. Lu exploited C<sub>2</sub>O<sub>4</sub><sup>2-</sup> as a traceless linchpin to perform cross-coupling reactions of electron-deficient alkenes (Scheme 2).<sup>[21–22]</sup> The latter occurs via a two-step cascade photoredox process initiated by the addition of the CO<sub>2</sub><sup>•-</sup> (generated upon visible light photoredox oxidative fragmentation of C<sub>2</sub>O<sub>4</sub><sup>2-</sup>) to an alkene **3** to provide a hydrocarboxylated intermediate **4**. Decarboxylation affords a C-centered radical **II**, which adds to a second alkene substrate **5** eventually affording cross-coupling products **6**. A dual photocatalyst system to selectively activate C<sub>2</sub>O<sub>4</sub><sup>2-</sup> and the carboxylate intermediate **4** relies on the use of

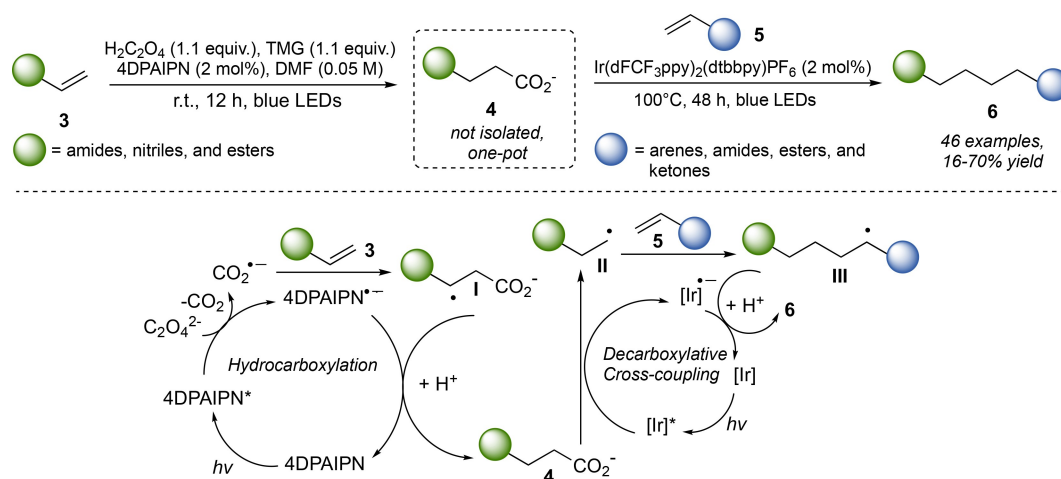
[a] Dr. C. Russo,\* C. Volpe,\* Dr. M. Giustiniano  
 Department of Pharmacy,  
 University of Naples Federico II,  
 Via D. Montesano 49, 80131, Napoli, Italy  
 E-mail: mariateresa.giustiniano@unina.it

[†] The authors contributed equally.

© 2025 The Author(s). ChemPhotoChem published by Wiley-VCH GmbH. This is an open access article under the terms of the Creative Commons Attribution License, which permits use, distribution and reproduction in any medium, provided the original work is properly cited.



Scheme 1. Reductive dehalogenation of 4-bromoanisole.



**Scheme 2.** Use of oxalate as a traceless linchpin for the reductive cross coupling of alkenes.

1,3-dicyano-2,4,5,6-tetrakis-(diphenylamino)-benzene (4DPAIPN) (2 mol%) and  $\text{Ir}(\text{dFCF}_3\text{ppy})_2(\text{dtbbpy})\text{PF}_6$  (2 mol%), respectively. The  $\text{C}_2\text{O}_4^{2-}$  was formed in situ by adding 1,1,3,3-tetramethylguanidine (TMG) (1.1 equiv.) as the base, since the use of cesium oxalate as the source of  $\text{CO}_2^{\cdot-}$  was less efficient due to solubility issues. Optimal reaction conditions for one-pot protocol featured *N,N*-dimethylformamide (DMF) as the solvent and irradiation with two 50 W blue LED lamps ( $\lambda = 456$  nm). The hydrocarboxylation step occurs at room temperature, while the decarboxylative cross-coupling requires heating at 100 °C. As for the reaction scope  $\alpha,\beta$ -unsaturated amides were reacted with a range of  $\alpha,\alpha$ -biarylalkenes to afford the cross-coupling adducts in good yields (46 examples, 16–70% yield). Shortly after, A. Matsumoto, K. Maruoka et al. reported a one-pot stepwise sequential photocatalytic process to access 1,4-dicarbonyls **10** from alkenes **3** and **5** by harnessing a formyl-stabilized phosphonium ylide **7** as an ambiphilic radical linchpin serving

as both a nucleophilic and an electrophilic C-centered radicals' source (Scheme 3).<sup>[23]</sup> The first step, leading to carbonyl derivative **8**, relies on the formation of radical **II** followed by its addition to a Michael acceptor **3** and requires an oxidizing photocatalyst, with 4CzIPN identified as the best performing one (Scheme 3). As for the second step, the need for a reducing photocatalyst is overcome by harnessing  $\text{CO}_2^{\cdot-}$  as a strong SET reductant, whose formation from an oxalate salt is promoted, indeed, by an oxidizing photocatalyst. Accordingly, the Authors showed that the addition of oxalic acid promoted the formation of an oxalate phosphonium salt **IV** from ylide **8**, able to quench the excited state 4CzIPN\* to undergo oxidative fragmentation to  $\text{CO}_2^{\cdot-}$  and  $\text{CO}_2$ . The former acts as a reductant to promote the formation of the radical intermediate **VI**, which adds to alkene **5** to afford an intermediate giving the products **10** upon HAT. A 20 mol% of methyl thiosalicylate **9** was necessary to promote the HAT to 1,4-dicarbonyl adduct **10**, under irradiation



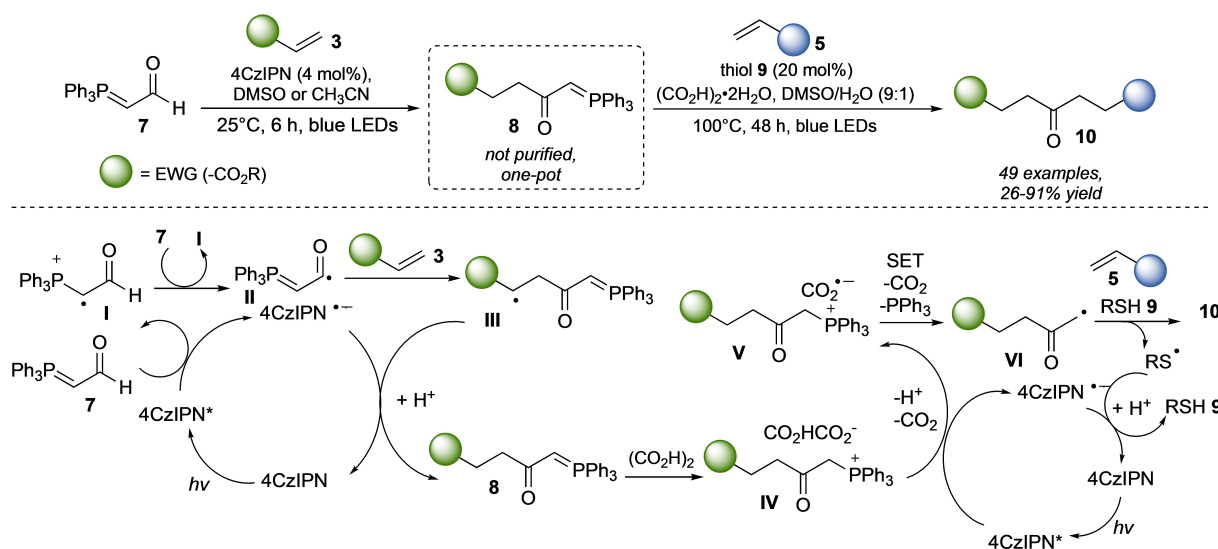
Camilla Russo obtained her PhD in Pharmaceutical Sciences in 2024 from the University of Naples Federico II, where she is currently working as a research fellow. Her research focuses on the development of green synthetic methodologies for the obtainment of drug-like bioactive scaffolds, with particular interest in isocyanide chemistry and visible-light photocatalysis.



Mariateresa Giustiniano is an Associate Professor at the University of Naples-Federico II, Department of Pharmacy. Her research interests focus on multicomponent reactions, visible-light photocatalysis, and medicinal chemistry.



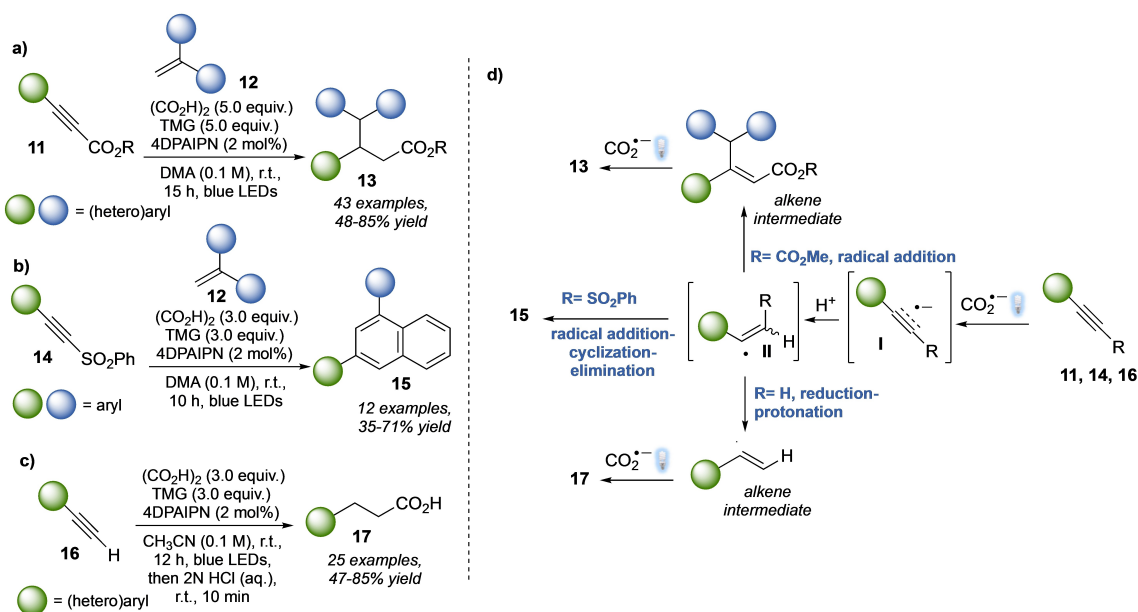
Carmine Volpe graduated summa cum laude in 2023 in Chemistry and Pharmaceutical Technologies at the University of Naples 'Federico II', where he is currently a research fellow working on the synthesis of multitarget agents against glioblastoma and on the development of new synthetic methodologies.



Scheme 3. Synthesis of 1,4-dicarbonyls from alkenes.

with blue LEDs ( $\lambda = 448$  nm). The reaction scope was illustrated by 39 compounds with yields in the range 26–83% and an exquisite functional group tolerance towards halogens, ester, carbamate, carbonyl, sulfonyl, phosphonate, hydroxyl, silyl, amide, and ethers (including a ring-strained epoxide). Furthermore, a set of ten structurally complex derivatives (60–91% yields) were synthesized from alkene derivatives of biorelevant scaffolds including for example deoxycholic acid, ibuprofen, vinclozolin, the carbohydrates *D*-glucofuranose and *D*-galactose, and amino acids such as *L*-proline, *L*-cysteine, and *L*-serine. As shown by J. Wu et al., the strong reducing properties of CO<sub>2</sub><sup>•-</sup> can be harnessed to achieve the photoredox catalytic reductive functionalization of aryl alkynes **11**, **14**, and **16** via the

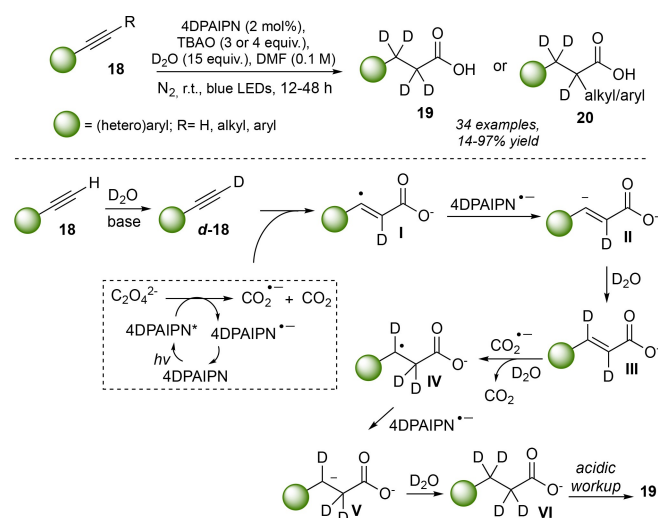
formation of alkyne radical anions **I** (Scheme 4).<sup>[24]</sup> More in detail, the tetramethylguanidium salt of oxalic acid, generated in situ (3–5 equiv. of both H<sub>2</sub>C<sub>2</sub>O<sub>4</sub> and TMG), undergoes oxidative degradation to CO<sub>2</sub><sup>•-</sup> and CO<sub>2</sub> upon reductive quenching of the excited photocatalyst 4DPAIPN (2 mol%). The reaction was run in DMA (0.1 M), at room temperature for 15 hours, and under blue LEDs irradiation ( $\lambda = 456$  nm). Depending on the alkyne substitution patterns, different adducts **13**, **15** and **17** can be obtained (Scheme 4a, b, and c, respectively). As for the reaction mechanism, the photogenerated CO<sub>2</sub><sup>•-</sup> forms, upon SET, an alkyne radical anion **I**, whose protonation affords a vinyl radical intermediate **II** (Scheme 4d). The latter can undergo different fates, such as radical addition



Scheme 4. Photoredox catalytic reductive functionalization of aryl alkynes.

to an alkene to finally afford hydroalkylated products **13**, upon consecutive SET reduction of the olefin intermediate (Scheme 4a). Alternatively, in the presence of an aryl sulfonyl moiety, the radical addition can be followed by a cyclization-elimination sequence to afford arylalkenylated products **15** (Scheme 4b). With terminal alkynes, the vinyl radical intermediate **II** undergoes reduction-protonation to give an alkene intermediate, and further nucleophilic addition of the  $\text{CO}_2^{\bullet-}$  enables the formation of hydrocarboxylated adducts **17** (Scheme 4c). The substrate scope (75 examples, 35–85%) revealed an exquisite functional group tolerance, while the synthetic value of the developed procedure was further probed in the modification of complex bioactive scaffolds such as citronellol, myrtenol, and *D*-glucose as well as in the gram scale synthesis of the anti-inflammatory drug Nabumeton by high-speed circulation flow. At the same time, L. Yin, D. Guo, X. Zhu et al. showed that by irradiating with blue LEDs ( $\lambda = 450$  nm) alkynes **18** in DMF, in the presence of 4DPAIPN (2 mol%) ( $E_{\text{red}}^* = -1.53$  V vs SCE),  $(\text{nBu}_4\text{N})_2\text{C}_2\text{O}_4$  (TBAO, 3 or 4 equiv.), and 15 equiv. of deuterium oxide ( $\text{D}_2\text{O}$ ), it is possible to get deuterocarboxylation derivatives **19** or **20** (Scheme 5).<sup>[25]</sup>

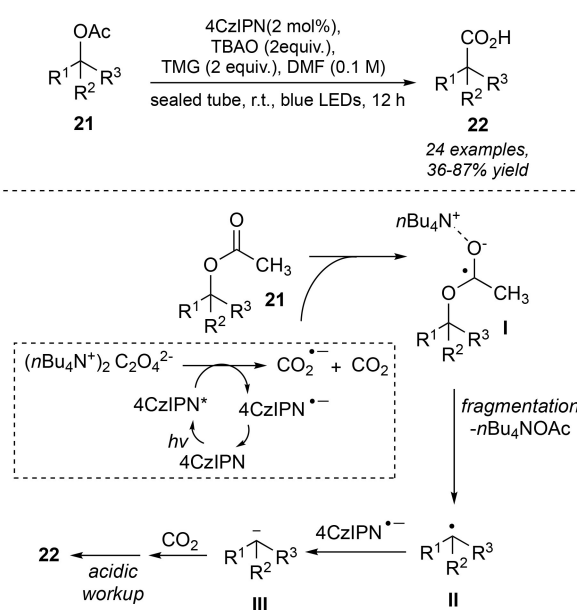
Mechanistically, the oxalate salt TBAO undergoes oxidative fragmentation to  $\text{CO}_2^{\bullet-}$  and  $\text{CO}_2$  upon photoinduced electron transfer (PET) by quenching the excited state 4DPAIPN\*. The  $\text{CO}_2^{\bullet-}$  adds to the  $d_1$ -alkyne **d-18** forming the vinyl radical intermediate **I**. The latter regenerates the ground-state photoredox catalyst, thus getting reduced to anion **II**. Deuteration of **II** leads to  $d_2$ -alkene **III**, undergoing reduction by means of SET mediated by  $\text{CO}_2^{\bullet-}$  and deuteration to **IV**. Further reduction of **IV** (by either 4DPAIPN\* or  $\text{CO}_2^{\bullet-}$ ), provides **V**, finally deuterated to carboxylate **VI**. Acidic work-up (HCl solution) affords the final carboxylic acids **19**. Reaction conditions enabled a 4 mmol scale deuterocarboxylation of ethynylbenzene to  $d_4$ -propionic acid in 71% yield. The reaction scope was broad (34 examples, 14–97% yields), with high efficiencies of *d*-incorporation (78–99%) and tolerated functional groups involving fluorine, nitrile, ester, ether, aromatic amine, and free carboxylic acid.



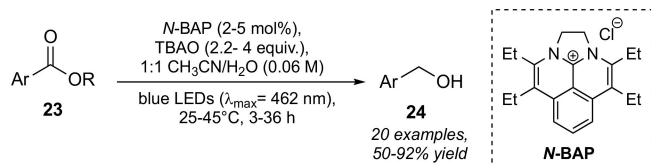
Scheme 5. Photoredox catalytic deuterocarboxylation of alkynes.

A similar photoredox catalytic set up (4 CzIPN (2 mol%) and TBAO (2 equiv.), in the presence of TMG as a base (2 equiv.)) was reported shortly after by X. Zhu et al. to engage acylated alcohols **21** in a deoxygenative carboxylation reaction (Scheme 6).<sup>[26]</sup> Differently from the previous reports, here, the  $\text{CO}_2$  generated upon oxidative fragmentation of TBAO is not merely waste, but acts as an electrophilic C1 source, while  $\text{CO}_2^{\bullet-}$  is key to reduce via SET the acylated alcohols **21** (Scheme 6).

Indeed, the distonic radical anion **I** undergoes fragmentation to give the alkyl radical **II**, which gets reduced to carbanion **III** upon regeneration of the ground-state photoredox catalyst. Interestingly, the interaction of **I** with the counterion of the oxalate salt was shown to be crucial to promote the  $\beta$ -fragmentation to **II**, with the tetrabutylammonium (TBA) being the only one to enable satisfactory yields, probably by forming stable ion pairs with the anion **III** and thus favoring carboxylation over protonation. Additionally, the use of oxalate as  $\text{CO}_2^{\bullet-}$  precursor was key to get carboxylated adducts, since the use of formate salts in the presence of a HAT catalyst afforded only deoxygenated products due to the rapid HAT quenching of the C-centered radical intermediate.<sup>[27]</sup> A library of twenty-four examples (36–87% yields) accounted for the good substrate scope including the synthesis of the anti-inflammatory drugs ibuprofen, naproxen, and flurbiprofen (74, 75%, and 78% yields, respectively) from their acyl alcohol precursors. More recently, Y. Uozumi et al. harnessed ammonium oxalate as a traceless reductant to achieve a 4-electron reduction of aromatic esters **23** to benzyl alcohols **24** promoted by a diazabenzacenaphthenium photocatalyst *N*-BAP under irradiation with 40 W blue LEDs ( $\lambda_{\text{max}} = 462$  nm), in a 1:1 MeCN- $\text{H}_2\text{O}$  solvent mixture, at 45 °C (Scheme 7).<sup>[28]</sup> The reaction scope involved twenty aromatic esters (methyl-, ethyl-, isopropyl-, and phenyl- derivatives), with yields ranging from 92% to 50% and

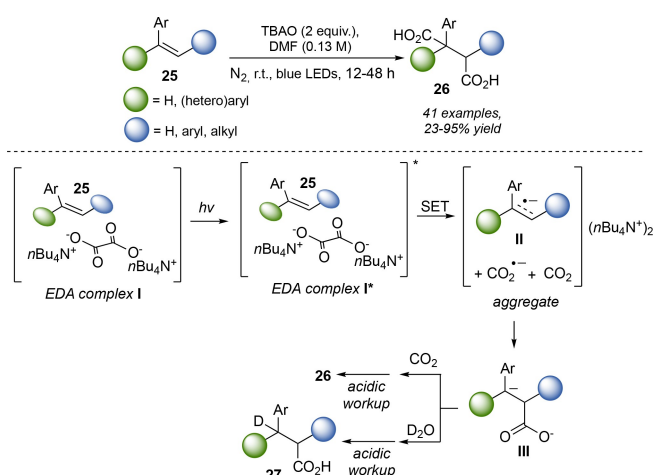


Scheme 6. Photoredox catalytic deoxygenative carboxylation of acylated alcohols.

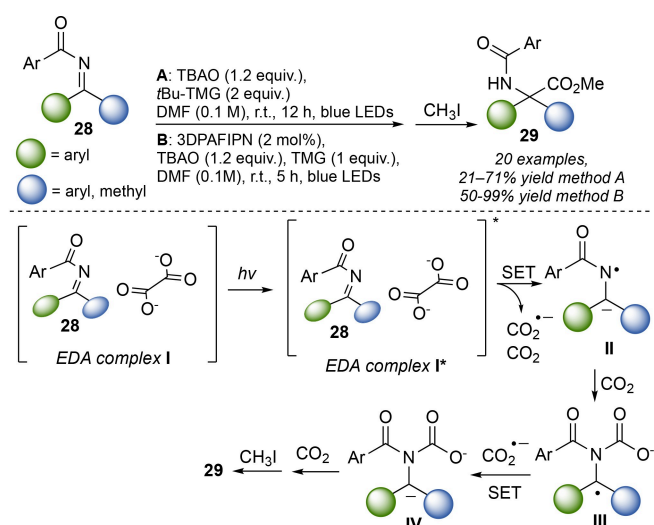


**Scheme 7.** Photoredox catalytic reduction of aromatic esters to benzyl alcohols.

electron-rich substrates such as methyl 4-methoxybenzoate being unreactive (0% yield) under the developed conditions, probably due a very negative reduction potential.



**Scheme 8.** Carboxylative 1,2-difunctionalization of alkenes via EDA complex formation.



**Scheme 9.** Photoredox catalytic synthesis of  $\alpha$ -amino acid esters from *N*-benzoyl imines.

### 3. Oxalate Salts in the Formation of Electron Donor-Acceptor (EDA) Complexes

Tetrabutyl ammonium has shown to be a noninnocent counterion also in the formation of EDA complexes between TBAO and alkenes (Scheme 8).<sup>[29]</sup> More in detail, TBAO is able to form charge-transfer complexes **I** with aryl substrates via  $\pi$ -cation interactions (Scheme 8). Under irradiation with 450 nm blue LEDs a PET from  $\text{C}_2\text{O}_4^{2-}$  to the alkene substrate, thus inducing the formation of  $\text{CO}_2^{\bullet-}$  and  $\text{CO}_2$ , which can both add to a carbon-carbon double bond as in alkenes, dienes, trienes, and indoles to afford 1,2- and 1,4-dicarboxylic acid derivatives (41 examples, 23–95% yields). Mechanistically, the formation of the benzyl anion **III** was supported by deuterium labelling studies via formation of *d*-carboxylic acid derivative **27** (Scheme 8).

TBAO has been also reported in the formation of EDA complexes with *N*-benzoyl imines **28** (Scheme 9).<sup>[30]</sup> Similarly to the previous procedure by X. Zhu et al., it is  $\text{CO}_2$  to act as C1-source.<sup>[26]</sup> Here, the switch from oxalic acid (forming in situ a TMG salt) to TBAO enables to suppress the formation of the reduced amine while favoring the hydrocarboxylation to form unnatural  $\alpha$ -amino acids **29** (Scheme 9). Indeed, blue LEDs irradiation of a DMF solution of *N*-benzoyl imines **28** and TBAO, in the presence of *t*Bu-TMG as a base, at room temperature, for 12 hours, leads to the formation of the corresponding  $\alpha$ -amino acids **29** in moderate to good yields (20 examples, 21–71% method A). Alternatively, good to excellent yields (50–99%) can be achieved by using 3DPAFIPN (2 mol%) as a photoredox catalyst and TMG (1.0 equiv.) as a base (method B, Scheme 9). Unsuccessful substrates include monoarylbenzoyl imines and simple aryl or benzyl imines (the benzoyl moiety is key to confer an electron acceptor behavior to the imine). Mechanistically, the distonic radical anion **III** can be generated upon addition of  $\text{CO}_2$  to **II** followed by SET reduction mediated by  $\text{CO}_2^{\bullet-}$  to give **IV**. Addition of  $\text{CO}_2$  to **IV** and *N*-decarboxylation affords the amino acid derivatives isolated as the corresponding methyl esters **29**. Deuterium labelling studies led the Authors to exclude a radical-radical coupling between **II** and  $\text{CO}_2^{\bullet-}$ .

### 4. Oxalate Salts as Hole Scavengers

The photocatalytic reduction of organic compounds such as nitroaromatics is typically achieved by using methanol as both the solvent and the sacrificial electron donor, whose aim is to scavenge holes ( $h^+$ ) in heterogeneous photocatalytic systems and thus reducing the recombination within the particles.<sup>[31–34]</sup>

In 2009, H. Kominami et al. showed that oxalic acid can be considered as a “greener” hole scavenger as compared to methanol, since the latter forms toxic formaldehyde as the oxidized species (opposed to safer  $\text{CO}_2$ ). Oxalate ions, indeed, are oxidized by  $h^+$ , forming  $\text{CO}_2$  and  $\text{CO}_2^{\bullet-}$ , the latter being able to reduce nitrobenzene. Accordingly, the authors reported that the photocatalytic reduction of nitrobenzene to aniline in an aqueous suspension of titanium (IV) oxide ( $\text{TiO}_2$ ) particles (Degussa P25  $\text{TiO}_2$ ) was accomplished in 95% yield after 30

minutes under photoirradiation at wavelengths  $> 300$  nm by a high-pressure mercury arc (400 W) and at 25 °C. The use of oxalate salts was also previously shown to induce the photocatalytic reduction of nitrate in aqueous dispersions of  $\text{TiO}_2$ .<sup>[35,36]</sup> More recent applications include the hydrogenation of phenol to cyclohexanol over a Rhodium-loaded Titanium (IV) oxide photocatalyst.<sup>[37]</sup> Such phenol degradation was also selected as a model reaction to investigate the effects of different scavenger agents in heterogeneous photocatalysis.<sup>[38]</sup> D. Scheres Firak et al. reported that at pH around 3 as the optimal one, the oxalate dianion coordinates  $\text{Ti}^{4+}$  forming inner-sphere complexes which favor electron transfer to the conduction band of titanium atoms or to the photogenerated *holes*. Under visible light the oxalate- $\text{TiO}_2$  complexes ( $\text{C}_2\text{O}_4^{2-}-\text{TiO}_2$ ) can promote the decomposition of oxalate into  $\text{CO}_2$  and  $\text{CO}_2^{\bullet-}$  via direct electron transfer from the oxalate to the conduction band of a Titanium atom (the hole does not participate). Under UV(A) irradiation, the Authors observed homolytic cleavage of the oxalate, yielding 2 equivalents of  $\text{CO}_2^{\bullet-}$ , indicating that the charge transfer can occur between the ligands and the photogenerated *holes*.<sup>[39]</sup> Representative applications of oxalate salts as *hole* scavengers also involve graphene/semiconductor composites,<sup>[40]</sup>  $\text{AVO}_4$  ( $A = \text{Bi, Fe}$ )-Carbon nanofibers (CNFs) heterostructures for the degradation of Rhodamine B,<sup>[41]</sup> combined magnetic  $\text{Ag}/\text{Fe}_3\text{O}_4/\text{TiO}_2$  nanofibers (NFs)<sup>[42]</sup> and bimetallic Mn–Fe MOFs<sup>[43,44]</sup> for the photocatalytic reduction of Cr(IV).

## 5. Photolysis of Transition Metal Oxalate Complexes

The oxalate dianion  $\text{C}_2\text{O}_4^{2-}$  is known to be a ligand in coordination complexes with transition metals such as V(III), Mn(III), Cr(III), Tc(IV), Fe(III), Ru(III), Co(III), Rh(III), and Ir(III).<sup>[2]</sup> It has also been reported as a bridging ligand to form bi- and polynuclear complexes.<sup>[45,46]</sup> Transition metal oxalates are largely applied as energy storage materials.<sup>[47,48]</sup> Ferrioxalate  $\text{Fe}^{\text{III}}(\text{C}_2\text{O}_4)_3^{3-}$  is one of the most extensively investigated complex as it is naturally occurring and it is used as an actinometer to quantify photon flux thanks to its high absorbance and reaction quantum yield.<sup>[49,50]</sup> Its photolysis (UV light) generates  $\text{CO}_2^{\bullet-}$  able to reduce one more equivalent of ferrioxalate and to induce the mineralization (degradation) of dissolved organic matter (DOM) in natural waters and atmospheric aerosol particles.<sup>[51]</sup> The photolysis of ferrioxalate occurs via direct photoexcitation, followed by ligand-to-metal charge-transfer (LMCT) triggering iron reduction. The oxidized oxalate radical anion undergoes fragmentation to  $\text{CO}_2^{\bullet-}$  and  $\text{CO}_2$  via molecular steps as revealed by ultrafast laser-based spectroscopic studies, quantum mechanical simulations, and molecular dynamics.<sup>[52,53]</sup> Interestingly, ferrioxalate is characterized by a broad absorption band centered at  $\lambda_{\text{max}} = 260$  nm, spanning toward the red ( $\lambda \sim 500$  nm).<sup>[54,55]</sup> Notwithstanding these valuable features, applications of transition metal oxalate complexes in synthetic photochemistry still represent a gap in the literature opened for contributing new advancements in the field.

## 6. Summary and Outlook

Oxalate salts are cheap and available reagents in visible light photoredox catalysis, useful as an electron reservoir and a C1-source. Their redox potential enables a smooth oxidative fragmentation to  $\text{CO}_2^{\bullet-}$  and  $\text{CO}_2$  under mild conditions. Up-to-date literature relies on the exploitation of  $\text{CO}_2^{\bullet-}$  as a strong “dark” reductant able to engage substrates such as aryl bromides, alkenes, alkynes, acylated alcohols, and *N*-benzoyl imines. The  $\text{CO}_2^{\bullet-}$  either can react as a C1 source or it can behave as a traceless linchpin in the reductive cross-coupling of alkenes. Furthermore, its reductive properties can be harnessed to get carbanion intermediates, able to undergo carboxylation reaction with  $\text{CO}_2$ . Importantly, the generation of  $\text{CO}_2^{\bullet-}$  via oxidative fragmentation of an oxalate salt stands for a valuable alternative to hydrogen atom abstraction from formate salts when the presence of a HAT agent is not compatible with the other reaction substrates (both as the starting materials and products). Furthermore, oxalate salts stand for an efficient and cleaner source of electrons as compared to more common trialkylamines, with inert  $\text{CO}_2$  as the only by-product. Worthy of note, the poor solubility of inorganic oxalate salts (e.g., sodium and potassium) is overcome by using either organic-soluble salts (e.g., tetrabutylammonium) or by forming them in situ via deprotonation with an organic base (e.g., tetramethylguanidine). Finally, the photochemistry of transition metal oxalate complexes highlighted in section 5 lacks synthetic organic applications, which would further expand the targetable chemical space. All these features point towards the engagement of even more complex and challenging substrates and make oxalate salts as a herald of rich and fascinating chemistry.

## Acknowledgements

Open Access publishing facilitated by Università degli Studi di Napoli Federico II, as part of the Wiley - CRUI-CARE agreement.

## Conflict of Interests

The authors declare no conflict of interest.

**Keywords:** oxalate salts · carbon dioxide radical anion · visible light photoredox catalysis · C1-source · EDA complex

- [1] *A Treatise on Chemistry* (H. Enfield Roscoe, C. Schorlemmer), New York, New York, D. Appleton and Co., 1890, volume 3, part 2, p. 105.
- [2] K. V. Krishnamurthy, G. M. Harris, *Chem. Rev.* **1961**, *61*, 213–246.
- [3] *CRC Handbook of Chemistry and Physics* (Ed.: J. Rumble), 100<sup>th</sup> ed., CRC Press, **2019**.
- [4] V. R. Franceschi, P. A. Nakata, *Annu. Rev. Plant Biol.* **2005**, *56*, 41–71.
- [5] A. Verma, R. Kore, D. R. Corbin, M. B. Shiflett, *Ind. Eng. Chem. Res.* **2019**, *58*, 15381–15393.
- [6] Q. Ma, H. He, C. Liu, *Atmos. Environ.* **2013**, *69*, 281–288.
- [7] E. Schuler, M. Demetriou, S. N. Raveendran, G.-J. M. Gruter, *ChemSusChem*. **2021**, *14*, 3636–3664.
- [8] J. A. Gibbard, E. Castracane, A. J. Shin, R. E. Continetti, *Phys. Chem. Chem. Phys.* **2020**, *22*, 1427–1436.

- [9] C. M. Hendy, G. C. Smith, Z. Xu, T. Lian, N. T. Jui, *J. Am. Chem. Soc.* **2021**, *143*, 8987–8992.
- [10] W. Xiao, J. Zhang, J. Wu, *ACS Catal.* **2023**, *13*, 15991–16011.
- [11] T. Kai, M. Zhou, S. Johnson, H. S. Ahn, A. J. Bard, *J. Am. Chem. Soc.* **2018**, *140*, 16178–16183.
- [12] J. Majhi, G. A. Molander, *Angew. Chem. Int. Ed.* **2024**, *63*, e202311853.
- [13] F. Pina, Q. G. Mulazzani, M. Venturi, M. Ciano, V. Balzani, *Inorg. Chem.* **1985**, *24*, 848–851.
- [14] Y. AlSalka, O. Al-Madanat, M. Curti, A. Hakki, D. W. Bahnemann, *ACS Appl. Energ. Mater.* **2020**, *3*, 6678–6691.
- [15] D. R. Prasad, M. Z. Hoffman, Q. G. Mulazzani, M. A. J. Rodgers, *J. Am. Chem. Soc.* **1986**, *108*, 5135–5142.
- [16] M. Z. Hoffman, D. R. Prasad, *J. Photochem. Photobiol. A* **1990**, *54*, 197–204.
- [17] For a representative recent application see: J. Xu, J. Cao, X. Wu, H. Wang, X. Yang, X. Tang, R. W. Toh, R. Zhou, E. K. L. Yeow, J. Wu, *J. Am. Chem. Soc.* **2021**, *143*, 13266–13273.
- [18] S. Kim, G. Park, E. J. Cho, Y. You, *J. Org. Chem.* **2016**, *81*, 7072–7079.
- [19] F. Draper, E. H. Doeven, J. L. Adock, P. S. Francis, T. U. Connell, *J. Org. Chem.* **2023**, *88*, 6445–6453.
- [20] K. Bhattacharyya, P. K. Das, *J. Phys. Chem.* **1986**, *90*, 3987–3993.
- [21] Z. Wu, M. Wu, K. Zhu, J. Wu, Y. Lu, *Chem* **2023**, *9*, 978–988.
- [22] D. Mazzarella, L. Dell'Amico, *Chem* **2023**, *9*, 766–768.
- [23] A. Matsumoto, N. Maeda, K. Maruoka, *J. Am. Chem. Soc.* **2023**, *145*, 20344–20354.
- [24] X. Tong, Z. Wu, H. Ting Ang, Y. Miao, J. Wu, *ACS Catal.* **2024**, *14*, 9283–9293.
- [25] P. Xu, H.-Q. Jiang, H. Xu, S. Wang, H.-X. Jiang, S.-L. Zhu, L. Yin, D. Guo, X. Zhu, *Chem. Sci.* **2024**, *15*, 13041–13048.
- [26] C.-W. Xu, S.-Y. Yan, H. Xu, S. Wang, L.-Q. Gu, P. Xu, L. Yin, X. Zhu, *ACS Catal.* **2024**, *14*, 11967–11973.
- [27] O. P. Williams, A. F. Chmiel, M. Mikhael, D. M. Bates, C. S. Yeung, Z. K. Wickens, *Angew. Chem. Int. Ed.* **2023**, *62*, e202300178.
- [28] S. Okumura, S. Hattori, L. Fang, Y. Uozumi, *J. Am. Chem. Soc.* **2024**, *146*, 16990–16995.
- [29] S. Wang, P. Xu, Z.-T. Liu, Y.-Q. Liu, H.-Q. Jiang, T.-Z. Hao, H.-X. Jiang, H. Xu, X.-D. Cao, D. Guo, X. Zhu, *ACS Cent. Sci.* **2025**, *11*, 46–56.
- [30] W.-W. Liu, P. Xu, H.-X. Jiang, M. -Lei Li, T. -Zi Hao, Y.-Q. Liu, S.-L. Zhu, K.-X. Zhang, X. Zhu, *ACS Catal.* **2024**, *14*, 10053–10059.
- [31] F. Mahdavi, T. C. Bruton, Y. Li, *J. Org. Chem.* **1993**, *58*, 744–746.
- [32] J. L. Ferry, W. H. Glaze, *Langmuir* **1998**, *14*, 3551–3555.
- [33] O. V. Makarova, T. Rajh, M. C. Thurnauer, A. Martin, P. A. Kemme, D. Crokep, *Environ. Sci. Technol.* **2000**, *34*, 4797–4803.
- [34] H. Tada, T. Ishida, A. Takao, S. Ito, *Langmuir* **2004**, *20*, 7898–7900.
- [35] Y. Li, F. Wasgestian, *J. Photochem. Photobiol. A* **1998**, *112*, 255–259.
- [36] H. Kominami, A. Furusho, S. Murakami, H. Inoue, Y. Kera, B. Ohtani, *Catal. Lett.* **2001**, *76*, 31–34.
- [37] A. Kinoshita, K. Nakanishi, R. Yagi, A. Tanaka, K. Hashimoto, H. Kominami, *Appl. Catal. A* **2019**, *578*, 83–88.
- [38] J. T. Schneider, D. Scheres Firak, R. R. Ribeiro, P. Peralta-Zamora, *Phys. Chem. Chem. Phys.* **2020**, *22*, 15723–15733.
- [39] C. B. Mendive, T. Bredow, J. Schneider, M. Blesa, D. Bahnemann, *J. Catal.* **2015**, *322*, 60–72.
- [40] M.-Q. Yang, C. Han, Y.-J. Xu, *Nanoscale* **2015**, *7*, 18062–18070.
- [41] Y. Guan, Y. Su, J. Mu, L. Wang, H. Li, X. Li, H. Che, Z. Guo, *J. Mater. Sci. Mater. Electron.* **2018**, *29*, 11852–11861.
- [42] Y.-H. Chang, M.-C. Wu, *Catalysts* **2019**, *9*, 72.
- [43] Z. Garazhian, A. Farrokhi, A. Rezaeifard, M. Jafarpour, R. Khani, *RSC Adv.* **2021**, *11*, 21127–21136.
- [44] N. Tan Luong, K. Hanna, J.-F. Boily, *J. Catal.* **2024**, *432*, 115425.
- [45] V. M. Masters, C. A. Sharrad, P. V. Bernhardt, L. R. Gahan, B. Moubaraki, K. S. Murray, *J. Chem. Soc. Dalton Trans.* **1998**, 413–416.
- [46] M. Clemente-León, E. Coronado, C. Martí-Gastaldo, F. M. Romero, *Chem. Soc. Rev.* **2011**, *40*, 473–497.
- [47] J. S. Yeoh, C. F. Armer, A. Lowe, *Mater. Today Energy* **2018**, *9*, 198–222.
- [48] A. K. Singh, P. Jaiswal, P. Singh, *Iop. Conf. Ser. Mater. Sci. Eng.* **2021**, *1166*, 012032.
- [49] D. M. Mangiante, R. D. Schaller, P. Zarzycki, J. F. Banfield, B. Gilbert, *ACS Earth Space Chem.* **2017**, *1*, 270–276.
- [50] I. P. Pozdnyakov, O. V. Kel, V. F. Plyusnin, V. P. Grivin, N. M. Bazhin, *J. Phys. Chem. A* **2008**, *112*, 8316–8322.
- [51] Z. Luo, Y. Min, L. Qu, Y. Song, Y. Hong, *Chemosphere* **2021**, *265*, 129070.
- [52] Y. Ogi, Y. Obara, T. Katayama, Y.-I. Suzuki, S. Y. Liu, N. C.-M. Bartlett, N. Kurahashi, S. Karashima, T. Togashi, Y. Inubushi, K. Ogawa, S. Owada, M. Rubešová, M. Yabashi, K. Misawa, P. Slaviček, T. Suzuki, *Struct. Dyn.* **2015**, *2*, 034901.
- [53] L. Longetti, T. R. Barillot, M. Puppini, J. Ojeda, L. Poletto, F. van Mourik, C. A. arrell, M. Chergui, *Phys. Chem. Chem. Phys.* **2021**, *23*, 25308–25316.
- [54] A. M. May, J. L. Dempsey, *Chem. Sci.* **2024**, *15*, 6661–6678.
- [55] X. Li, M. Hou, Y. Fu, L. Wang, Y. Wang, D. Lin, Q. Li, D. Hu, Z. Wang, *Chin. Chem. Lett.* **2023**, *34*, 107752.

Manuscript received: December 16, 2024

Revised manuscript received: January 23, 2025

Accepted manuscript online: January 27, 2025

Version of record online: ■■■, ■■■

## REVIEW

---

Oxalate salts have been harnessed in synthetic organic photochemistry as C1-synthons, SET-reductants, and *hole* scavengers. Recent applications focused on reductive functionalizations are herein highlighted.



*Dr. C. Russo, C. Volpe, Dr. M. Giustiniano\**

1 – 9

**The Multiple Facets of Oxalate Dianion in Photochemistry**